

EVOLUTION OF MICROSTRUCTURE AND MICROHARDNESS IN HPT TITANIUM DURING ANNEALING

A.P. Zhilyaev^{1,2}, S.N. Sergeev¹, V.A. Popov¹ and A.V. Orlov^{2,3}

¹Institute for Metals Superplasticity Problems, Khalturina 39, Ufa 450001, Russia

²Research Laboratory for Mechanics of New Nanomaterials, St. Petersburg State Polytechnical University, Polytechnicheskaya 29,, St. Petersburg 195251, Russia

³Institute of Problems of Mechanical Engineering, Russian Academy of Sciences, Bolshoy pr. 61, Vas. Ostrov, St. Petersburg 199178, Russia

Received: November 25, 2014

Abstract. Evolution of microstructure and microhardness in commercially pure titanium processed by high pressure torsion during annealing at 300, 350, 450, 650, and 750 °C for 10 minutes is analyzed. XRD and microhardness measurements were employed for the evaluation of strength and microstructural parameters (crystallite size and microstrain).

1. INTRODUCTION

Intense plastic deformation (or severe plastic deformation) is the novel method of enhancing mechanical properties of metals and alloys for advanced applications [1-3]. Highly strained metallic materials can possess not only an ultrafine-grained (UFG) structure but also specific nanostructural features [4-6]. To date, it is well established that bulk nanostructured materials (BNMs) can be processed successfully through microstructural refinement using two basic methods of intense plastic deformation: (i) high pressure torsion [7]; (ii) equal channel angular pressing [8]. Over the last decade, there emerged a wide variety of new techniques of intense plastic deformation such as (i) accumulative roll bonding (ARB) [9]; (ii) multiaxial forging [10]; twist extrusion [11]; and many others. Nevertheless HPT has remained the most popular approach, specifically as a method for processing model nanostructured materials in order to study their properties at laboratory scale.

Nanostructured Ti and its alloys are employed for biomedical applications [12-15]. Pure Ti pos-

sesses the highest biocompatibility with living organisms, but it has limited use in medicine due to its low strength. High-strength nanostructured pure Ti processed by intense plastic deformation opens new possibilities for biomedical application [3]. Toxic alloying elements are not present in the implants made of nanostructured Ti, and such implants exhibit better biocompatibility. Additionally, the implant size can be reduced to minimize surgical intervention. However, there is a new route for additional improvement of biomedical implants made of pure titanium by fabricating high-strength nano-Ti/ceramic composites for medical engineering. Typical processes such as physical vapor deposition comprises high temperature (typically between 150 and 500 °C) during coating. So, thermostability of pure titanium is most important property for use it in nanocomposites. Although there are a number of reports (see for references [6]) devoted to evolution microstructure and microtexture of titanium and Ti alloys during annealing one set of important experiments is need to be performed: evolution of nanostructure in titanium processed by HPT annealed at elevated temperature for short time com-

Corresponding author: A.P. Zhilyaev, e-mail: alexz@anrb.ru

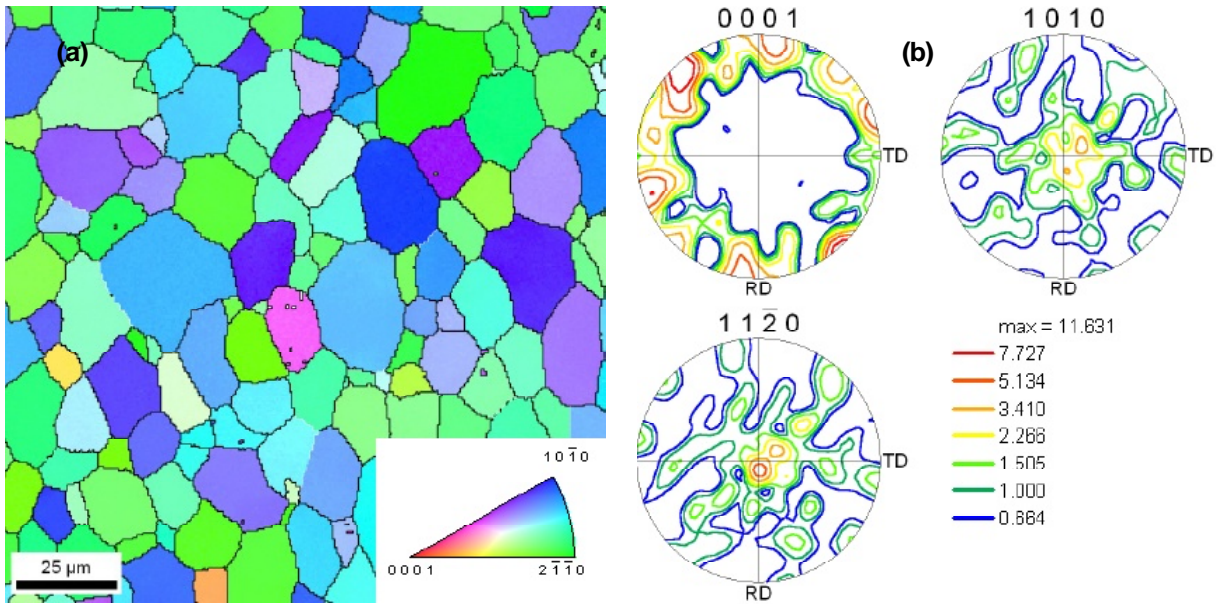


Fig. 1. IPF map (a) and pole figures (b) of commercially pure titanium prior HPT processing.

parable with one for fabricating Ni-ceramic composites.

2. MATERIALS AND EXPERIMENTAL PROCEDURE

Disks of commercial-purity titanium (designated in Russian nomenclature as VT1-0) which has a typical chemical composition (in wt.%: 0.12%O; 0.15%Fe, 0.07%C; 0.04%N; 0.01%H; 0.05%Si, balance Ti) were annealed at 600 °C for one hour prior HPT processing. Measurements showed that the initial Vickers microhardness value was 175.5 ± 2.5 Hv. The HPT specimens were cut in the form of disks having diameters of 10 mm and thicknesses of about 1 mm. These disks were processed at room temperature by constrained HPT device under applied pressure, $P=6$ GPa and for total five full revolutions. Nanostructured Ti specimens were annealed in furnace for 10 minutes at temperatures of 300, 350, 450, 550, and 750 °C. The microhardness was measured along two diameters of all HPT disks with distances of 0.5 mm between each indentation. These measurements were taken using a PMT-3M microhardness tester equipped with a Vickers indenter. Values of H_v were documented under loads of 100 gf with the dwell time of 15 s.

The EBSD analysis of annealed titanium was performed using a TESCAN MIRA 3LMH FEG scanning electron microscope equipped with an EBSD scan step of 50 nm. The acquired data were subjected to standard clean-up procedures to a grain size of three pixels. The grain sizes were measured using the linear intercept as the distances between

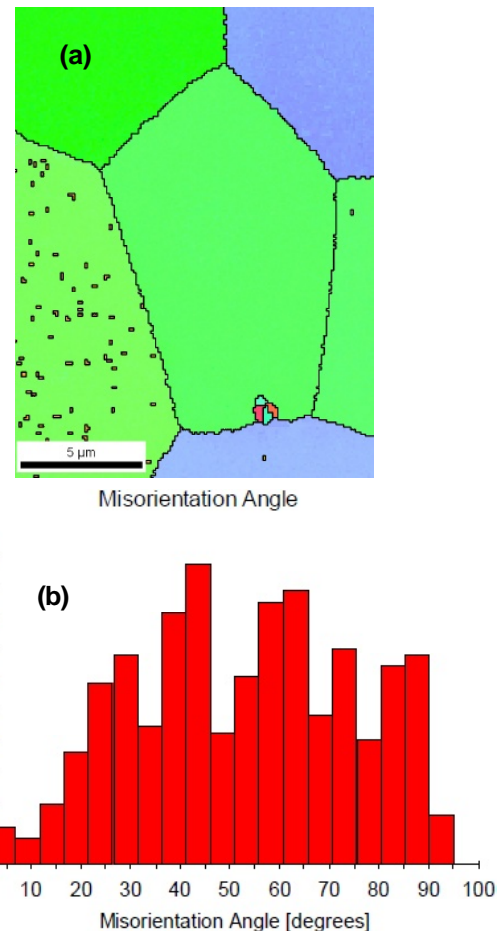


Fig. 2. High-resolution IPF map (a) and grain boundary misorientation distribution (b) of commercially pure titanium prior HPT processing.

high-angle grain boundaries with misorientations of 15° and more. Fig. 1 presents inverse pole figure (IPF) map and pole figures of annealed titanium.

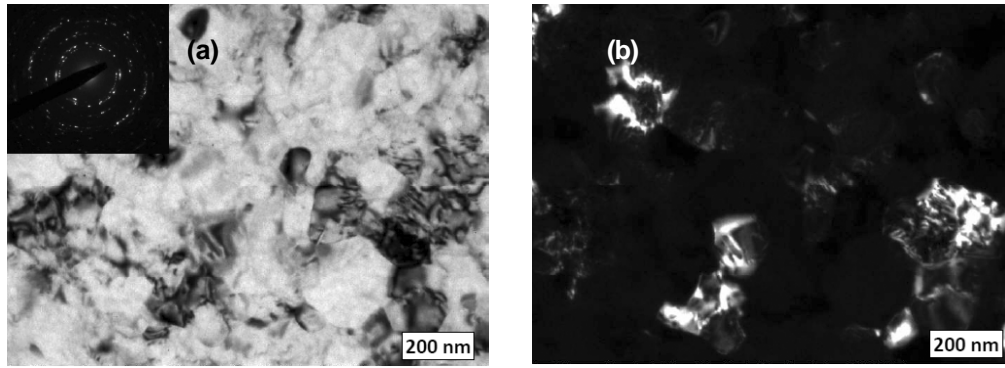


Fig. 3. TEM micrograph of HPT processed titanium: (a) bright field and (b) dark field. Inset shows SAED.

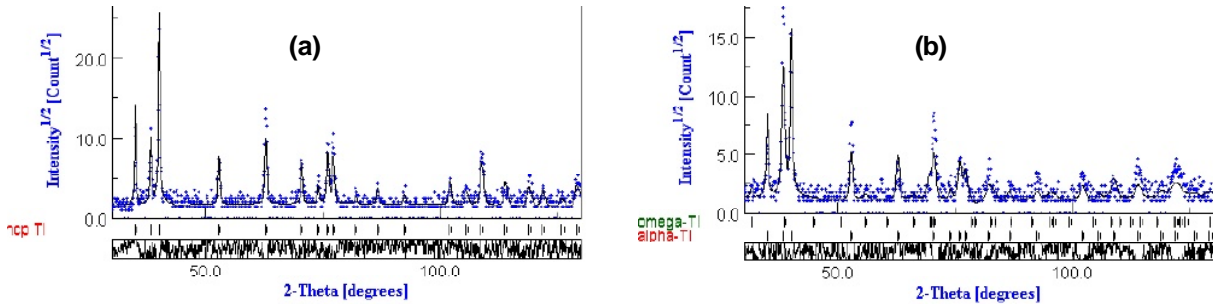


Fig. 4. XRD plot of (a) annealed and (b) HPT processed titanium.

Mean grains size of annealed titanium was 15.0 ± 1.5 μm . Texture is typical for extruded titanium with basal plane (0001) parallel to normal direction (long axis of extruded rod). Fig. 2 shows high-resolution IPF map of few grains (Fig. 2a) and grain boundary misorientation distribution (Fig. 2b). One can see that grains have equilibrium 120° triple junctions, and dislocation-free grains are separated mostly by high-angle grain boundaries (Fig. 2b).

Transmission electron microscopy (JEOL) was employed to characterize fine microstructure of nanostructured titanium processed by HPT. Fig. 3 depicts bright field (Fig. 3a) and dark field images. Inset in Fig. 3a shows selected area diffraction pattern taken from the area of ~ 0.5 μm . Bright field image (Fig. 3a) demonstrates highly non-equilibrium structure of HPT titanium. With dark field image (Fig. 3b), one evaluates the mean grain size of NC titanium to be about 200 nm or less.

The XRD analyses were undertaken by DRON-3 instrument equipped with monochromator using Cu radiation ($K_{\alpha 1} = 1.54060$ \AA). The scan step was 0.02° , and the delay time was 2.5 s. Rietveld analysis using MAUD software [16] was performed in order to monitor the microcrystallite size, d , and the microstrain, $\langle \varepsilon^2 \rangle^{1/2}$. An example of fitted experimental and calculated X-ray profiles is given in Fig. 4 where it is evident that the calculated curve is in good agreement with the experimental points. Unprocessed titanium samples have only alpha phase. After HPT deformation some amount of omega phase

appears. The omega phase is unstable, and, after heating to 250 – 300 $^\circ\text{C}$, the omega-to-alpha transformation occurs. In specimens annealed at higher temperatures, no traces of omega phase were detected.

3. RESULTS AND DISCUSSION

3.1. Microhardness evolution

Nanostructured titanium processed by high pressure torsion possesses homogeneous microhardness distribution along diameter of the disk specimen (Fig. 5a) with average value of around 281.8 ± 12.1 Hv which is in good agreement with reported earlier [17–19]. Fig. 5b presents an evolution of microhardness measured at half-radius of the HPT disk annealed at temperatures of 300, 350, 450, 650, and 750 $^\circ\text{C}$ for 10 minutes. Strength of HPT titanium drops down drastically for specimens annealed at 650 and 750 $^\circ\text{C}$. A trend line (Fig. 5b) indicates that after annealing at 500 $^\circ\text{C}$ microhardness would be about 260 Hv. This value in excellent agreement with the microhardness value of 256 Hv reported in [19] for HPT titanium annealed at 500 $^\circ\text{C}$ for 10 minutes.

3.2. XRD analysis

Fig. 6 demonstrates evolution of crystallite size, d , and microstrain in HPT specimens subjected to annealing. Crystalline size and microstrain increase

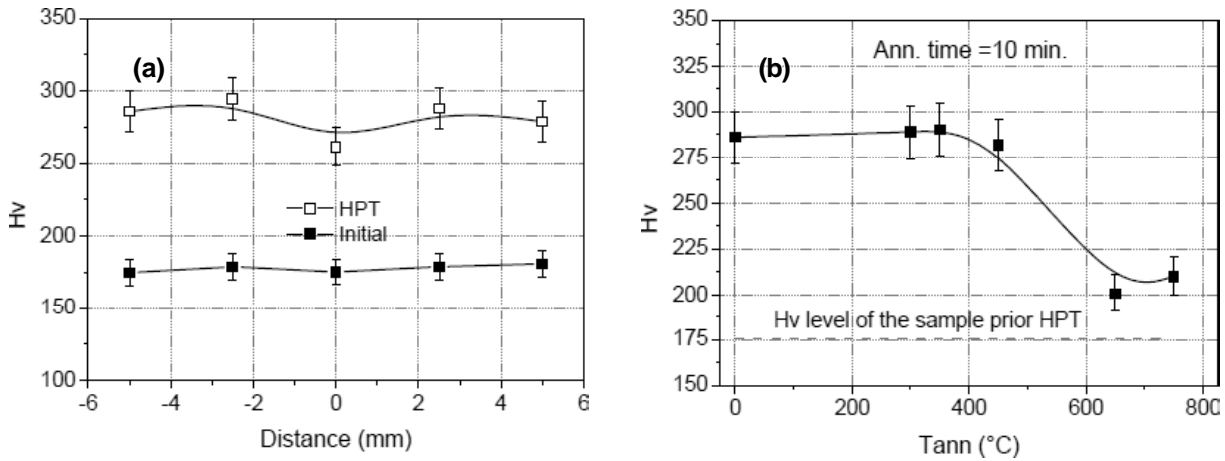


Fig. 5. Microhardness as a function of (a) distance from the center of the Ti disk and (b) annealing temperature.

non-monotonically with increase in annealing temperature. Each of these values has a local maximum for the HPT titanium annealed at 450 °C. These maxima indicate that nanostructured titanium has a crystallite size of ~100 nm and high level of microstrain. With the following relationship [20] between the microstrain $\langle \varepsilon^2 \rangle^{1/2}$ and the dislocation density ρ : $\rho = 3^{1/2} \cdot \langle \varepsilon^2 \rangle^{1/2} / (d \cdot b)$ (where d is the crystallite size, and b is the Burgers vector for alpha-Ti), one can plot the value of the dislocation density as a function of annealing temperature (Fig. 7). The dislocation density has a local maximum at $T = 500$ °C. This phenomenon can explain a paradox of “high strength – high ductility” observed in annealed HPT titanium and reported in Ref. [17].

4. CONCLUDING REMARKS

High-pressure torsion was used to produce significant grain refinement in CP Ti. Grain size detected

by TEM was below 200 nm, crystallite size evaluated by XRD was about 50 nm. High level of microstrain and dislocation density were generated in CP Ti during high pressure torsion. Significant increase in crystallite size, decrease in both microhardness and microstrain were detected in HPT titanium specimen annealed at temperatures higher than 600 °C. Simultaneous increase in crystallite size and dislocation density was observed in nanostructured titanium annealed at $T \sim 500$ °C. It was established that HPT titanium is thermostable up to temperature ~ 600 °C for short time annealing (not longer than 10 minutes), and any processes for fabricating Ti-ceramic composites can be employed if they operate at the conditions indicated.

ACKNOWLEDGEMENTS

This work was supported by Russian Science Foundation under Grant #14-29-00199.

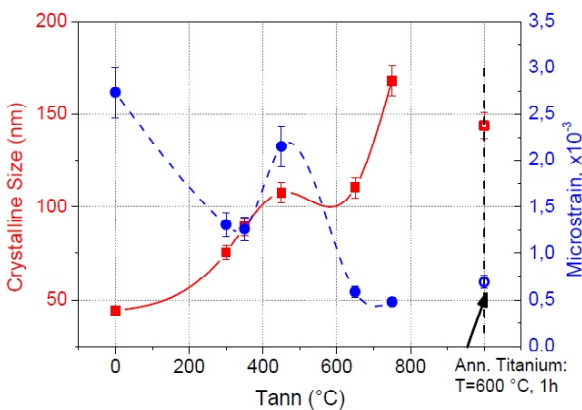


Fig. 6. Crystallite size and microstrain in HPT titanium are presented as functions of annealing time. In the right part of the map, experimental data for annealed initial titanium are shown.

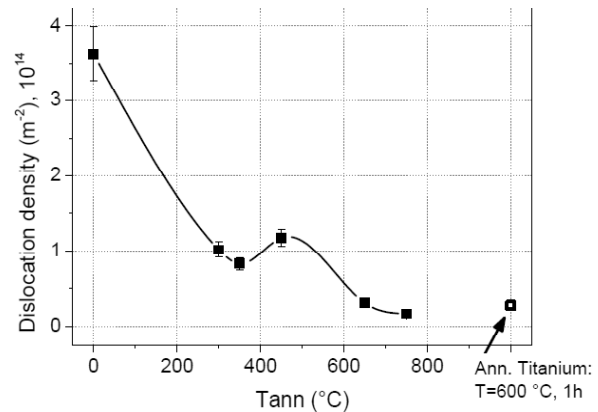


Fig. 7. Dislocation density in HPT titanium as a function of annealing temperature.

REFERENCES

- [1] R.Z. Valiev, R.K. Islamgaliev and I.V. Alexandrov // *Prog. Mater. Sci.* **45** (2000) 103.
- [2] H. Gleiter // *Acta Mater.* **48** (2000) 1.
- [3] R.Z. Valiev, I. Sabirov, A.P. Zhilyaev and T.G. Langdon // *JOM* **64** (2012) 1134.
- [4] B. Baretzky, M.D. Baró, G.P. Grabovetskaya, J. Gubicza, M.B. Ivanov, Yu.R. Kolobov, T.G. Langdon, J. Lendvai, A.G. Lipnitskii, A.A. Mazilkin, A.A. Nazarov, J. Nogues, I.A. Ovidko, S.G. Protasova, G.I. Raab, A. Revesz, N.V. Skiba, J. Sort, M.J. Starink, B.B. Straumal, S. Surinach, T. Ungar and A.P. Zhilyaev // *Rev. Adv. Mater. Sci.* **9** (2005) 45.
- [5] R.Z. Valiev, Y. Estrin, Z. Horita, T.G. Langdon, M.J. Zehetbauer and Y.T. Zhu // *JOM* **58** (2006) 33.
- [6] R.Z. Valiev, A.P. Zhilyaev and T.G. Langdon, *Bulk nanostructured materials: Fundamentals and applications* (New Jersey, Wiley & Sons, 2014).
- [7] A.P. Zhilyaev and T.G. Langdon // *Prog. Mater. Sci.* **53** (2008) 893.
- [8] R.Z. Valiev and T.G. Langdon // *Prog. Mater. Sci.* **51** (2006) 881.
- [9] Y. Saito, N. Tsuji, H. Utsunomiya, T. Sakai and R.G. Hong // *Scripta Mater.* **39** (1998) 1221.
- [10] O.R. Valiakhmetov, R.M. Galeev and G.A. Salishchev // *Fiz. Metall. Metalloved.* **10** (1990) 204.
- [11] D.V. Orlov, V.V. Stolyarov, H. Sh. Salimgareyev, et al., In: *Ultrafine Grained Materials III*, ed. by Y.T. Zhu, T.G. Langdon, R.Z. Valiev, S.L. Semiatin, D.H. Shin and T.C. Lowe (Warrendale (PA), TMS, 2004), p. 457.
- [12] S. Faghihi, A.P. Zhilyaev, J.A. Szpunar, F. Azari, H. Vali and M. Tabrizian // *Adv. Mater.* **19** (2007) 1069.
- [13] S. Faghihi, F. Azari, A.P. Zhilyaev, J.A. Szpunar, H. Vali and M. Tabrizian // *Biomaterials* **28** (2007) 3887.
- [14] R.Z. Valiev, I.P. Semenova, V.L. Latysh, H. Rack, T.C. Lowe, J. Petruzelka, L. Dluhos, D. Hrusak and J. Sochova // *Adv. Eng. Mater.* **10** (2008) B15.
- [15] Y. Estrin, E.P. Ivanova, A. Michalska, V.K. Truong, R. Lapovok and R. Boyd // *Acta Biomater.* **7** (2011) 900.
- [16] <http://www.ing.unitn.it/maud/>
- [17] R.Z. Valiev, A.V. Sergueeva and A.K. Mukherjee // *Scripta Mater.* **49** (2003) 669.
- [18] K. Edalati, E. Matsubara and Z. Horita // *Metall. Mater. Trans. A* **40** (2009) 2079.
- [19] C.T. Wang, N. Gao, M.G. Gee, R.J.K. Wood and T.G. Langdon // *Wear* **280-281** (2012) 28.
- [20] A.P. Zhilyaev, I. Shakhova, A. Belyakov, R. Kaibyshev and T.R. Langdon // *Wear* **305** (2013) 89.